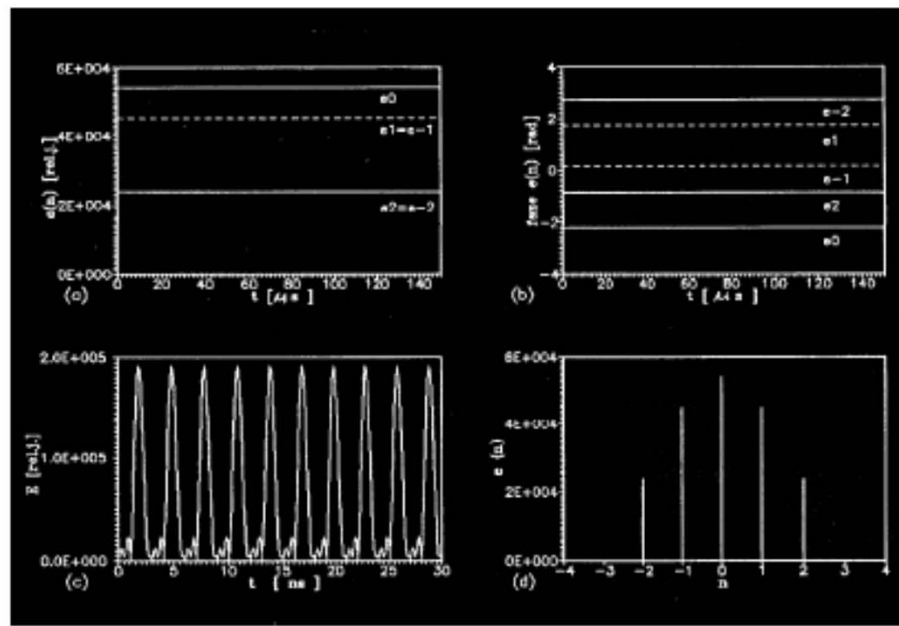


Aktivní ML

MODEL: 5 modes, Maxwell-Bloch equations (29 diff Eqs.)



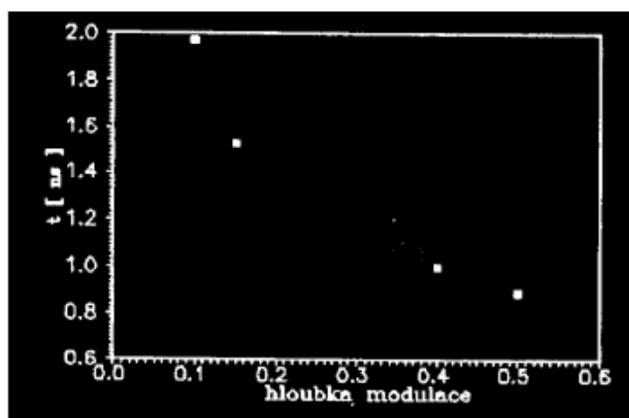
LOSS MODULATION:

$$\frac{1}{t_c} = K(1 + \theta \cos \omega t)$$

LASER Co:

MgF_2 , $\theta =$

0.5



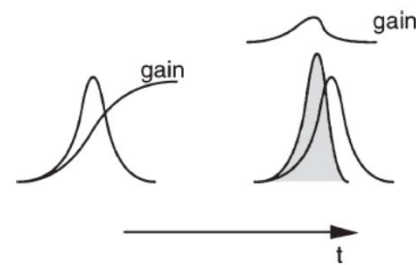
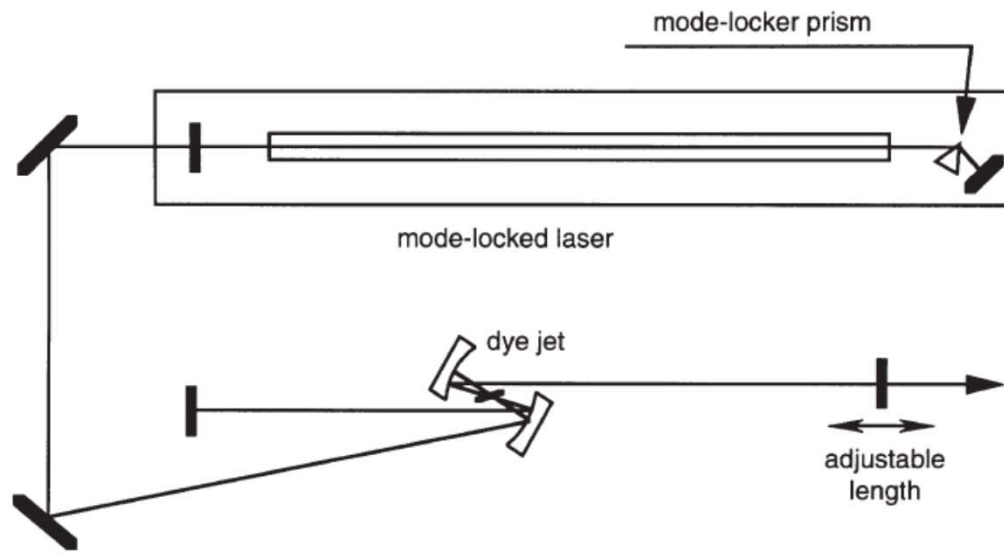


Fig. 4.6. Pulse shortening through gain saturation. *Left*, the time envelope of the pump pulses and the corresponding gain increase in the dye (in arbitrary normalized units). *Right*, result of the synchronized propagation of the dye oscillator pulse through the gain medium. The leading part of the pulse is strongly amplified up to the point when the gain saturates. The trailing part is not amplified, which results in a narrowing of the pulse [4.23–24]

Synchronní čerpání

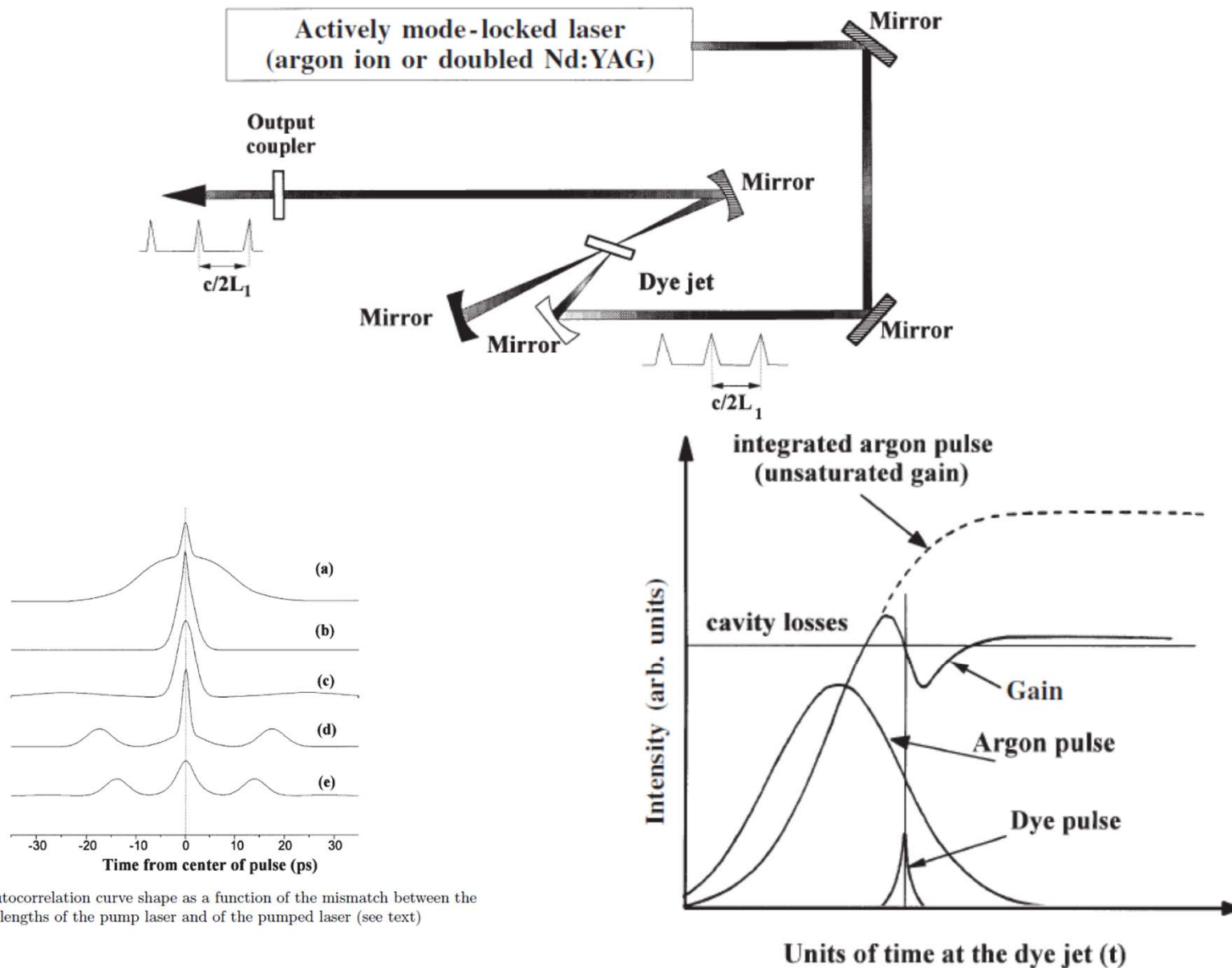
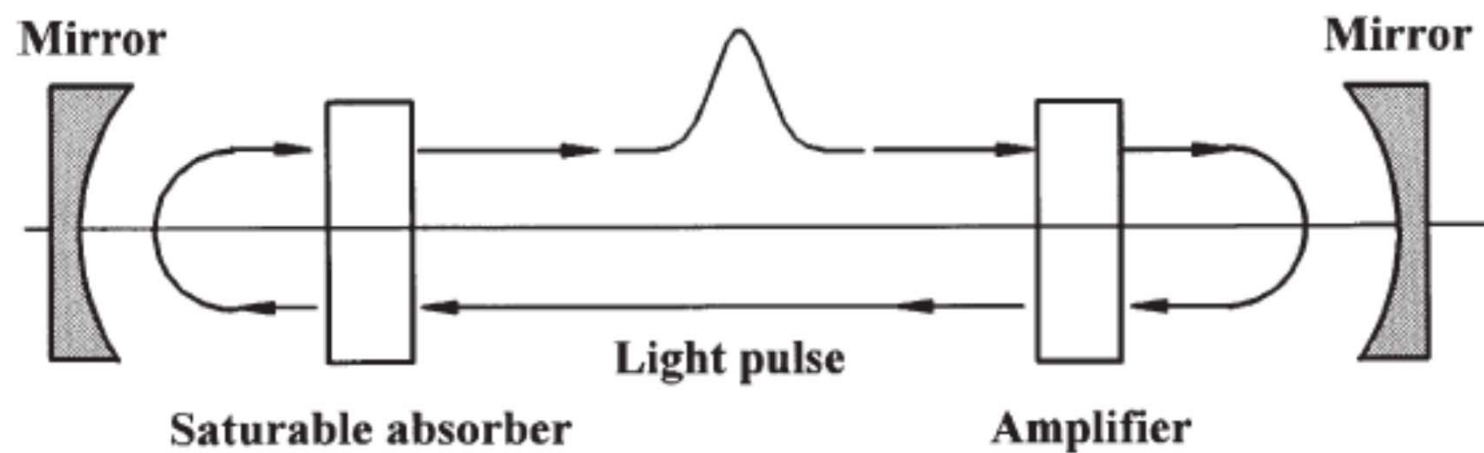


Fig. 3.11. Autocorrelation curve shape as a function of the mismatch between the cavity optical lengths of the pump laser and of the pumped laser (see text)



Pasivní ML

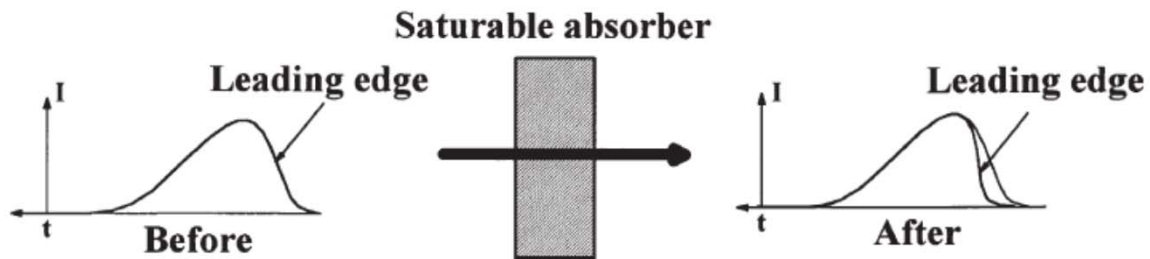


Fig. 3.15. Illustration of pulse shape modification after crossing a saturable absorber

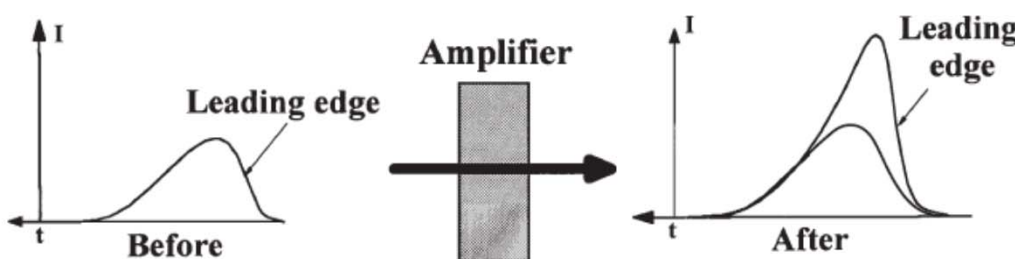
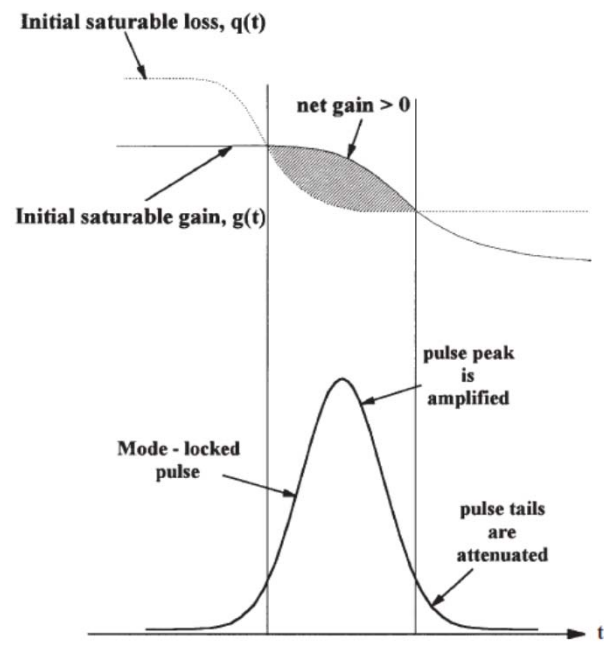
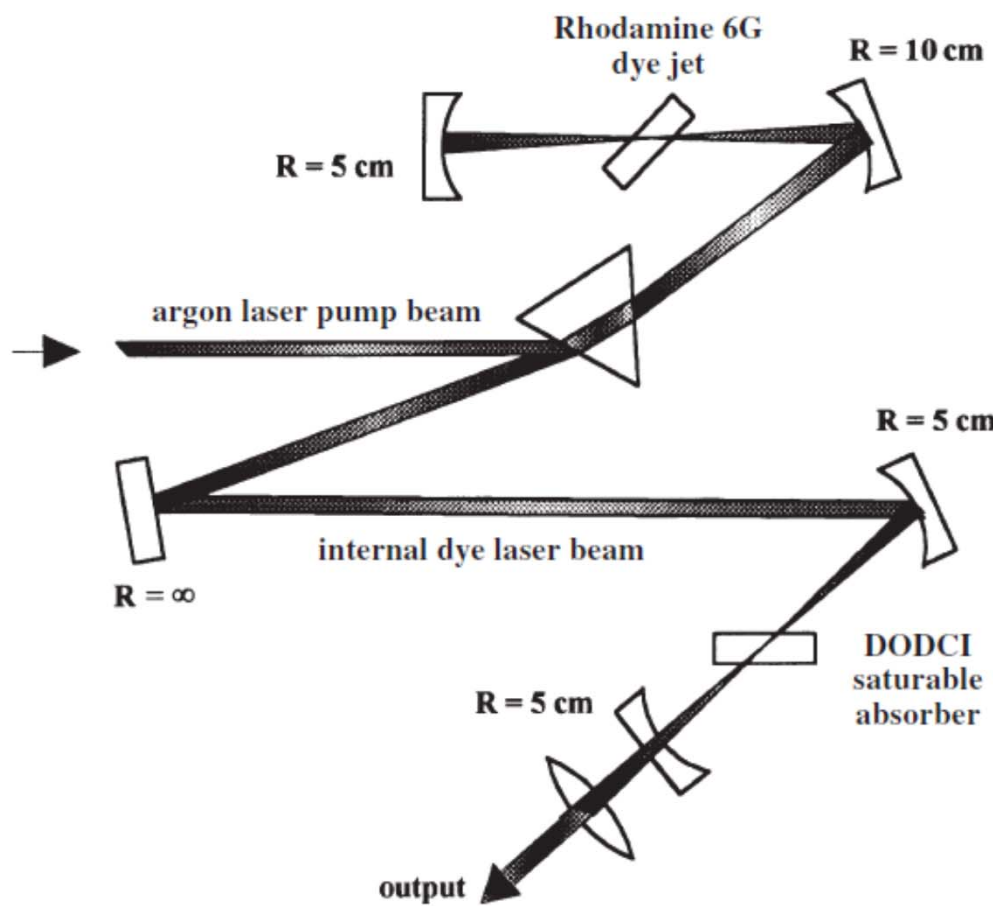


Fig. 3.16. Illustration of pulse shape modification after crossing an amplifying medium





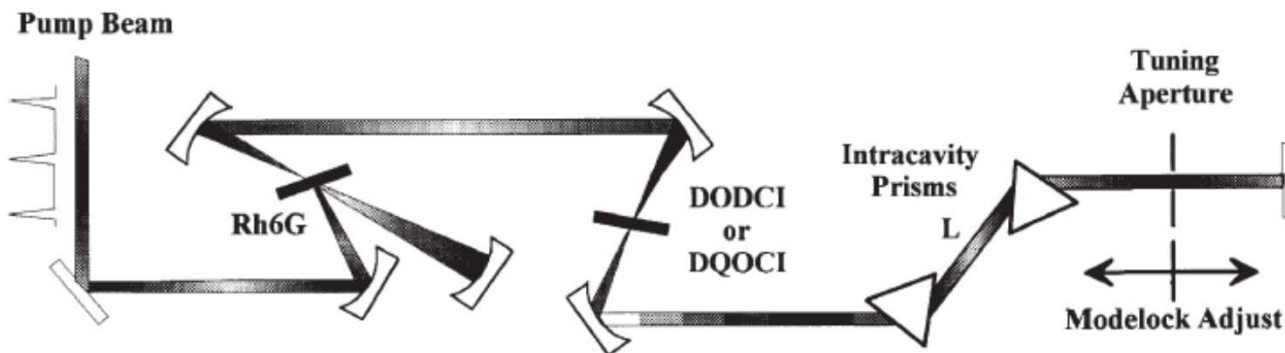
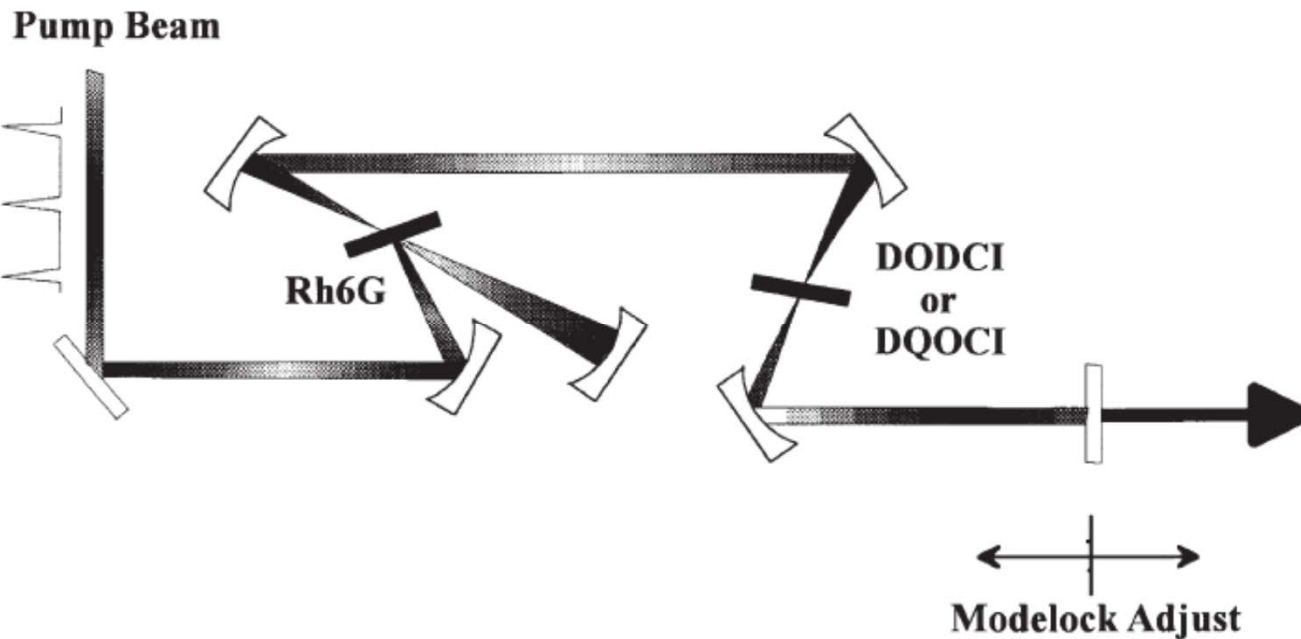
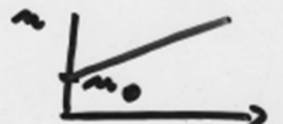


Fig. 3.21. Cavity design of hybrid mode-locked laser with inserted prisms for group velocity dispersion (GVD) compensation

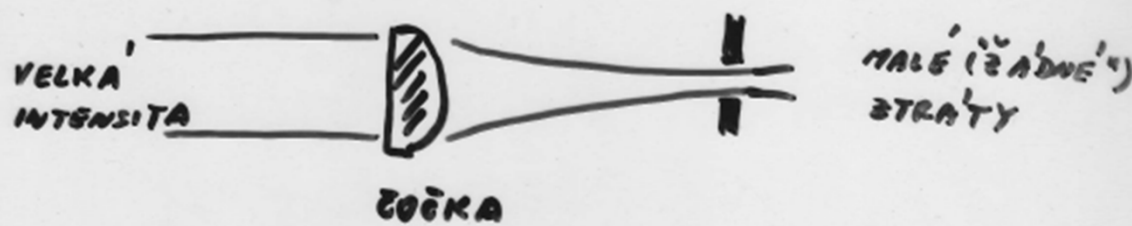
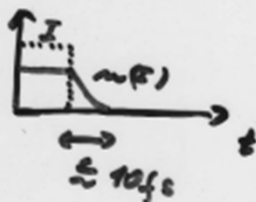
Hybridní ML

NELINEÁRNÍ OPTIKA

$$n(I) = n_0 + n_2 I$$



"RYCHLÉ"



ZOŠKA



DESTICKA

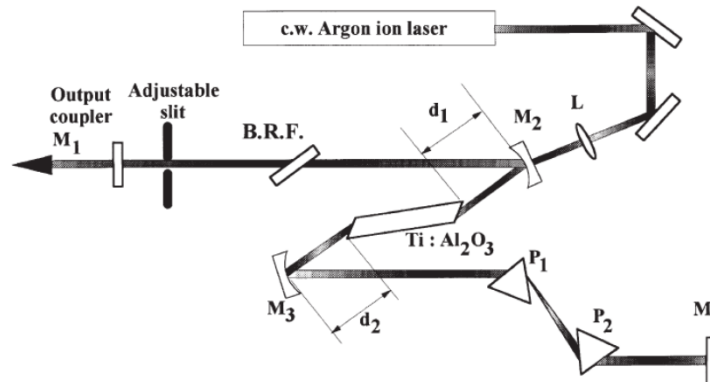


Fig. 3.23. Typical cavity design of a self-mode-locked Ti:sapphire laser using the KLM (Kerr lens mode-locking) process (see text)

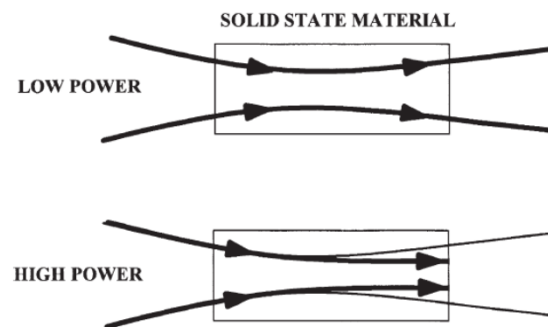


Fig. 3.24. Illustration of the self-focusing effect by the optical Kerr effect on the beam waist of a laser beam at high and low intensity

Kerr ML

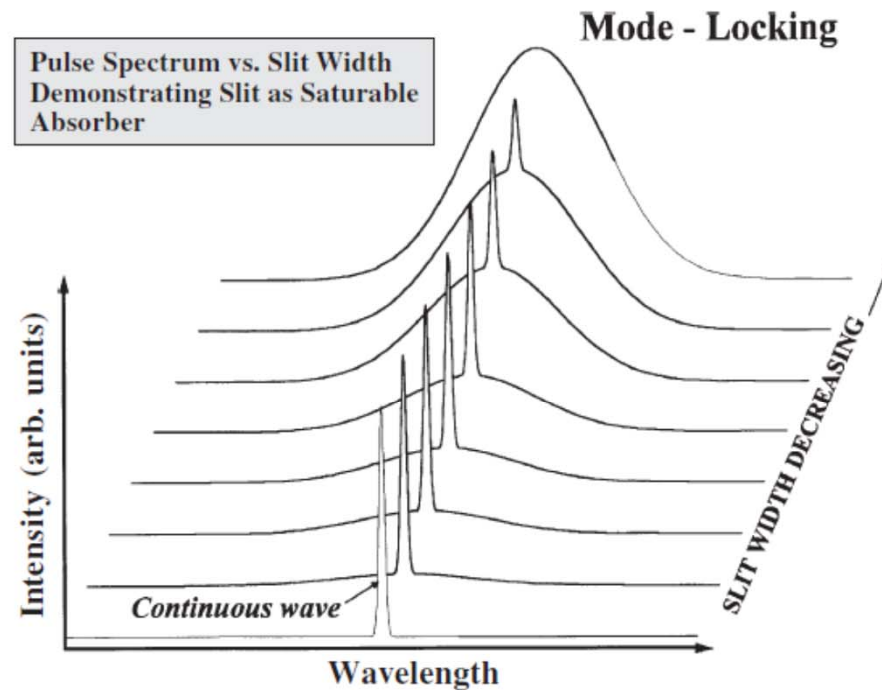


Fig. 3.25. Spectral distribution of laser output for different widths of the slit inserted in the cavity, which controls the mode-locking by the optical Kerr effect

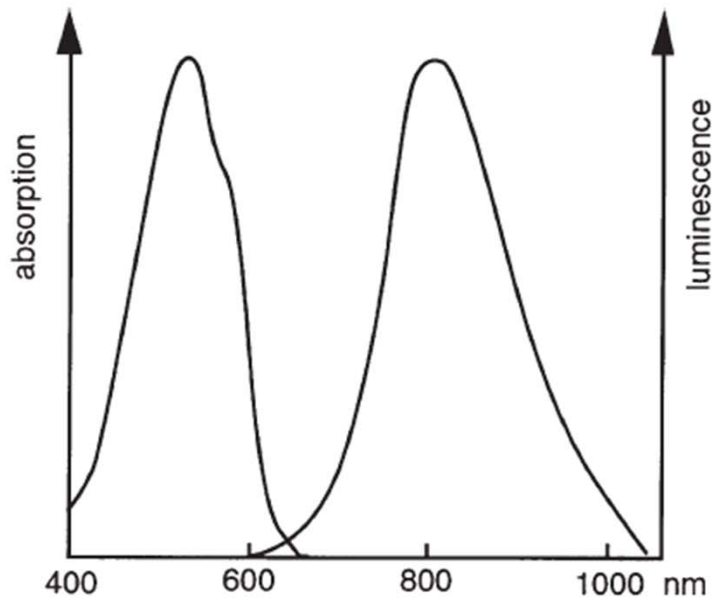


Fig. 4.15. Normalized absorption and emission spectra of Ti^{3+} ions embedded as impurities in a sapphire matrix ($\text{Ti:Al}_2\text{O}_3$)

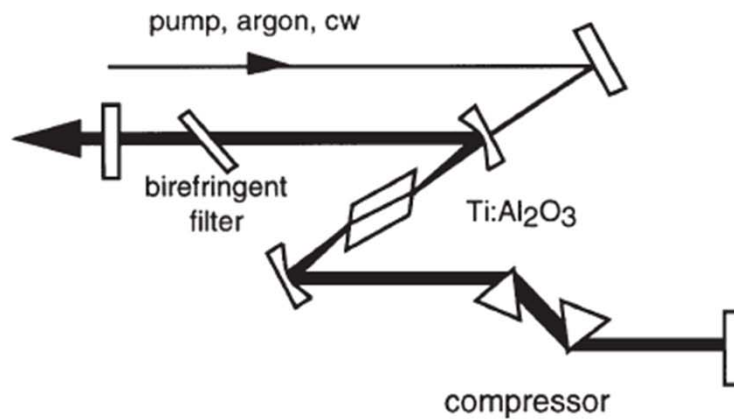


Fig. 4.16. Simplified sketch of a Ti:sapphire laser

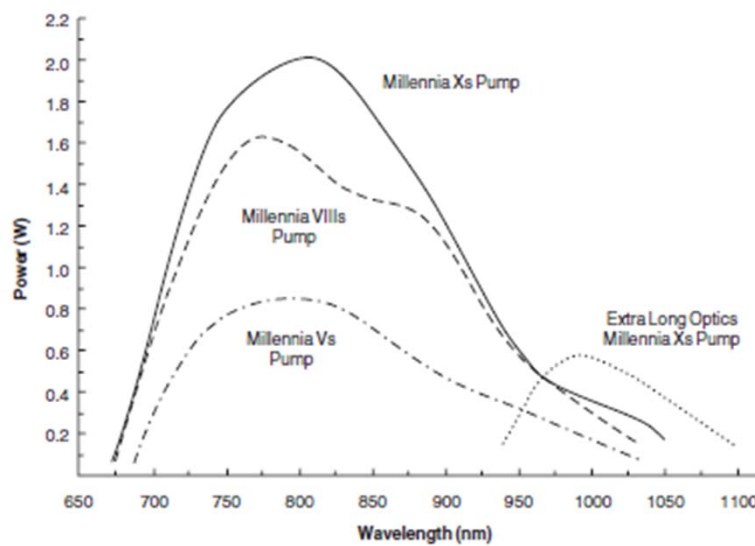


Figure 3-5: *Tsunami* femtosecond tuning curves for broadband optics when pumped by the various *Millennia* diode-pumped cw lasers shown.

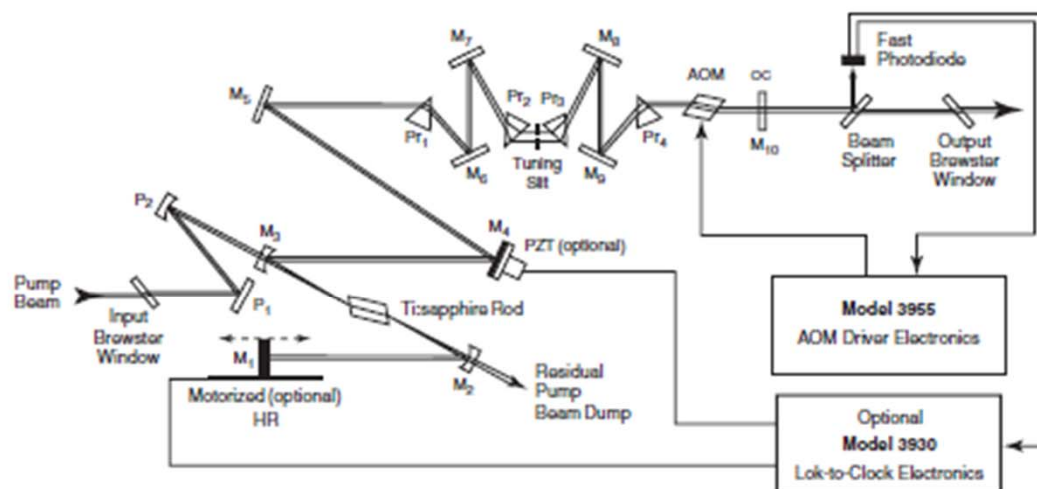
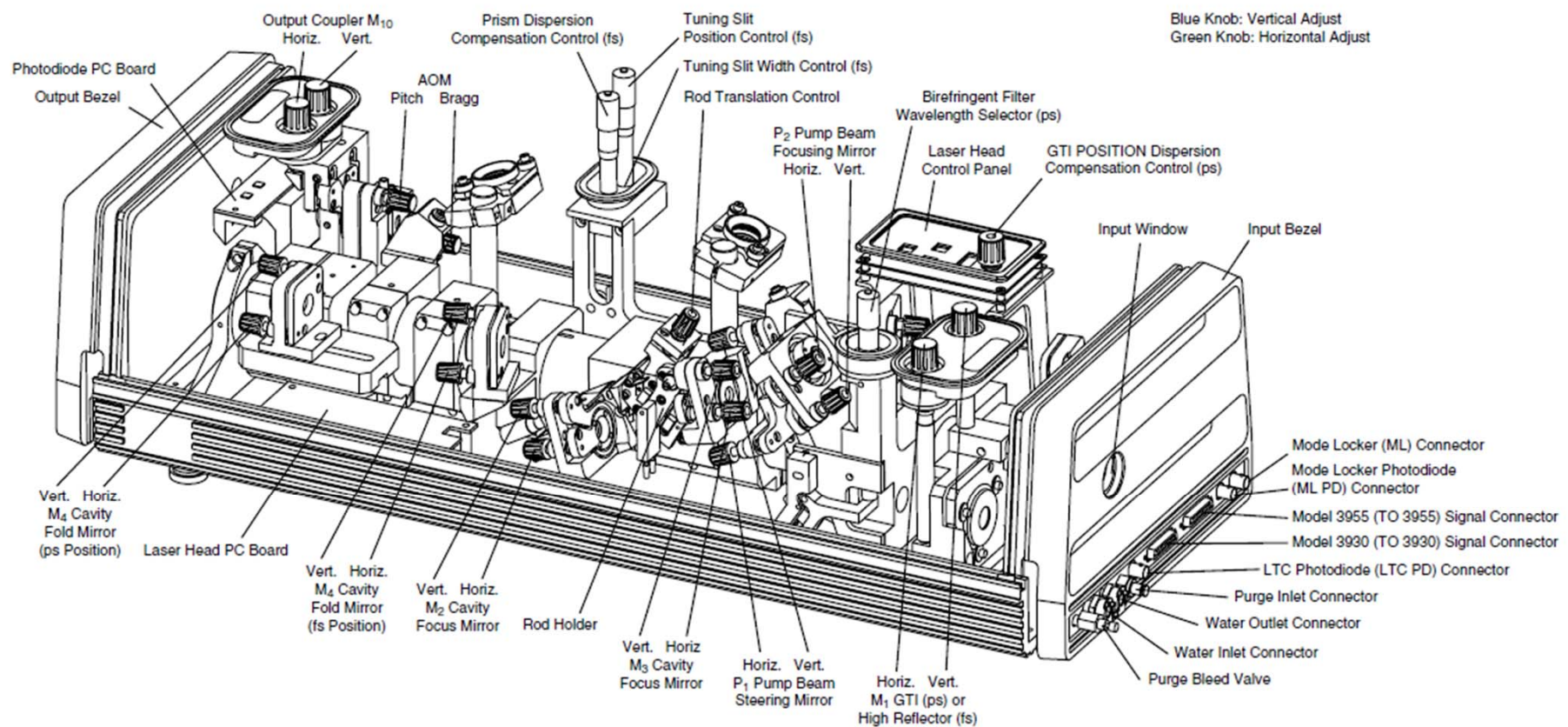
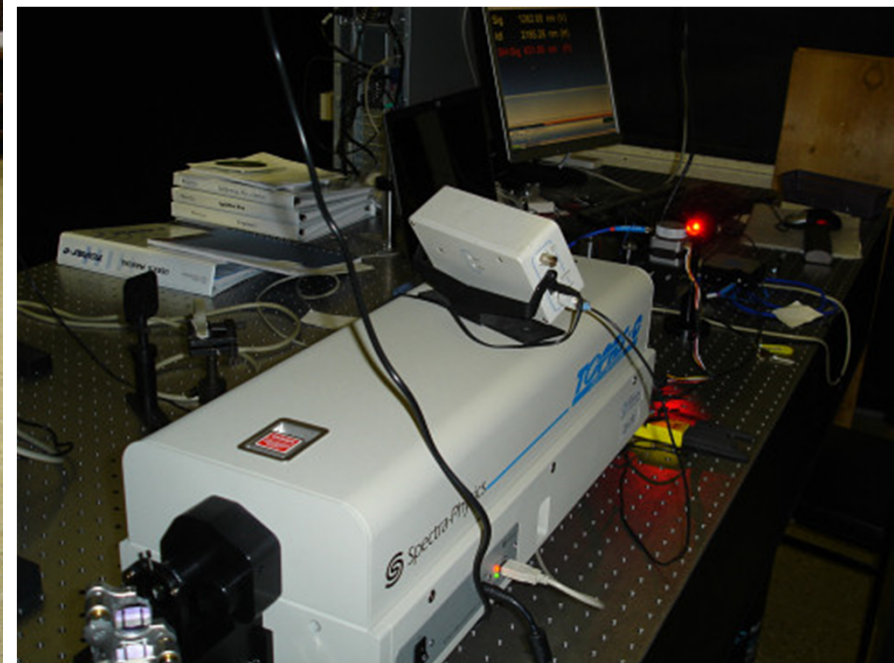
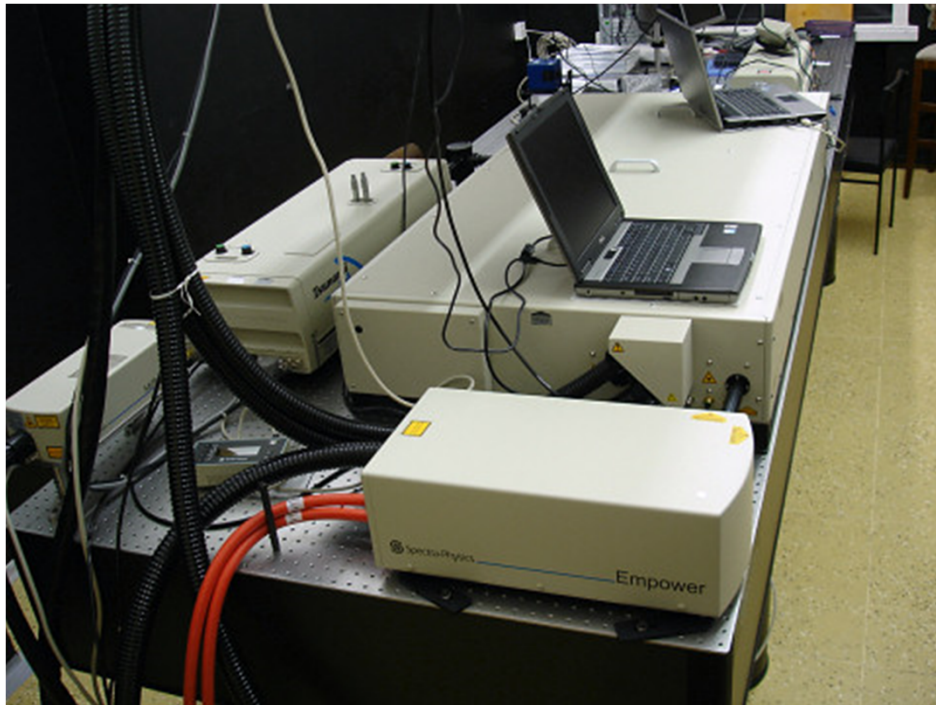


Figure 3-3: Beam Path for *Tsunami Models 3960 and 3941 Femtosecond Configurations*



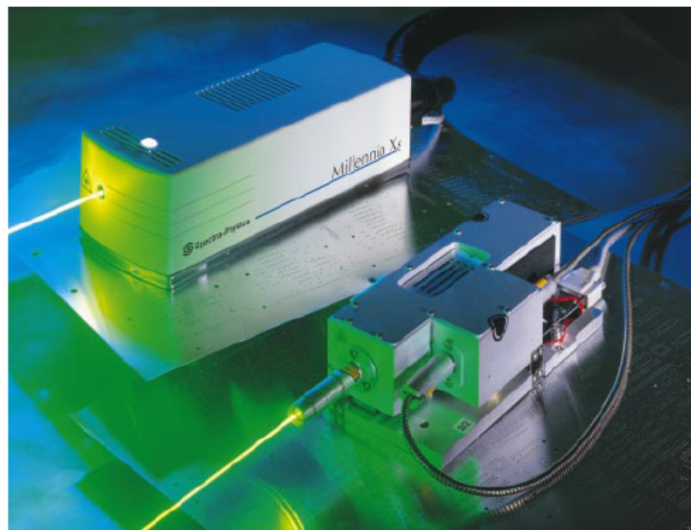


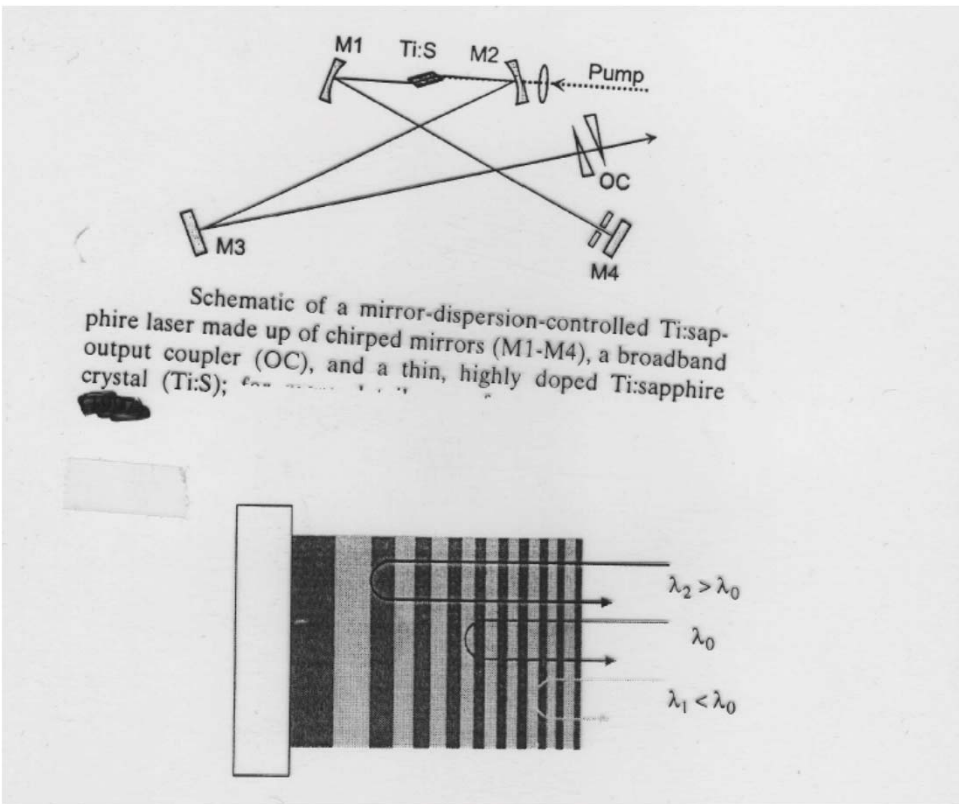
**Femtosekundová laboratoř- Ti:safírový laserový systém,
Spectra-Physics, 2007**

Čerpací lasery

Millenia: čerpací laser, cw, Nd:YVO₄, 5 W, SHG LBO 532 nm
(sám čerpán polovodičovými diodami na 809 nm)

Empower: čerpací laser, Q spínaný, Nd:YLF , > 20 mJ v pulsu 100 ns,
SHG LBO527 nm
(sám čerpán polovodičovými diodami na 809 nm)





Chirped mirrors

High-dispersive mirrors for femtosecond lasers

V. Pervak^{1*}, C. Teisset², A. Sugita², S. Naumov², F. Krausz^{1,2}, A. Apolonski^{1,2}

¹*Ludwig-Maximilians-Universität München, Am Coulombwall 1, D-85748 Garching, Germany*

²*Max-Planck-Institut für Quantenoptik, Hans-Kopfermann-Str. 1, D-85748 Garching, Germany*

*Corresponding author: volodymyr.pervak@mpq.mpg.de

JULY 2008 VOL 16, NO. 14 OPTICS EXPRESS

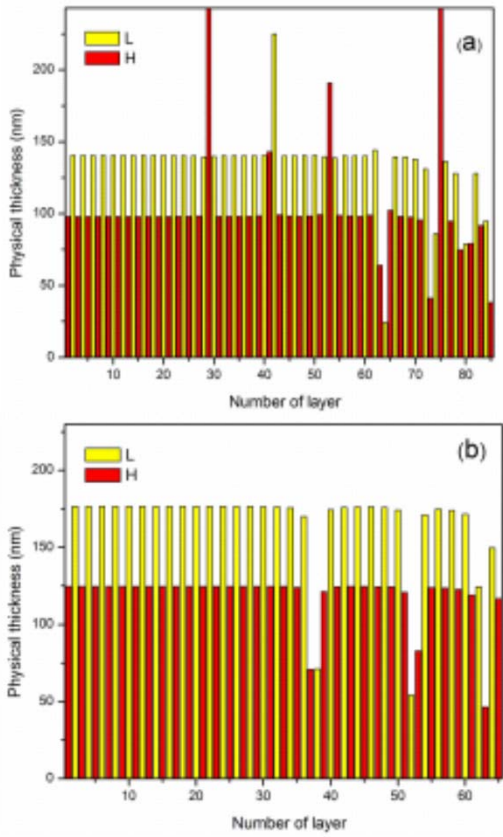


Fig. 1. The refractive index profile of HDMs. (a): HDM for Ti:Sa CPO, (b): for Yb:YAG oscillator.

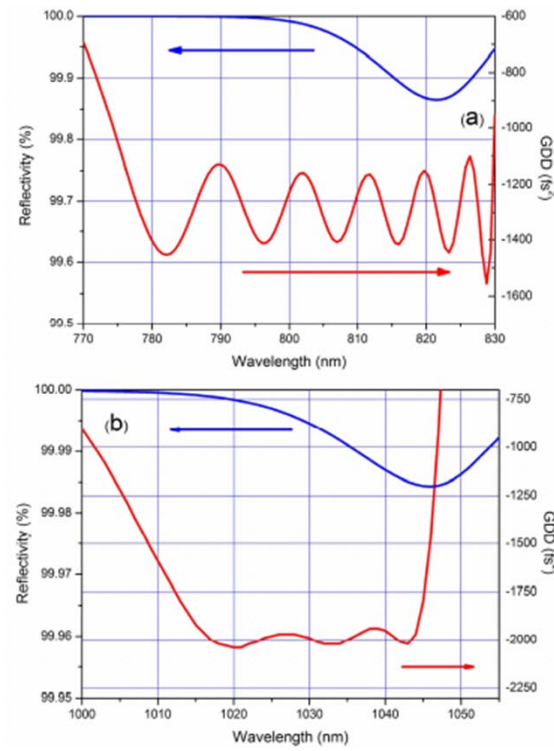


Fig. 2. The calculated GDD and reflectivity of HDMs. (a): HDM for Ti:sapphire CPO, (b): for Yb:YAG oscillator.

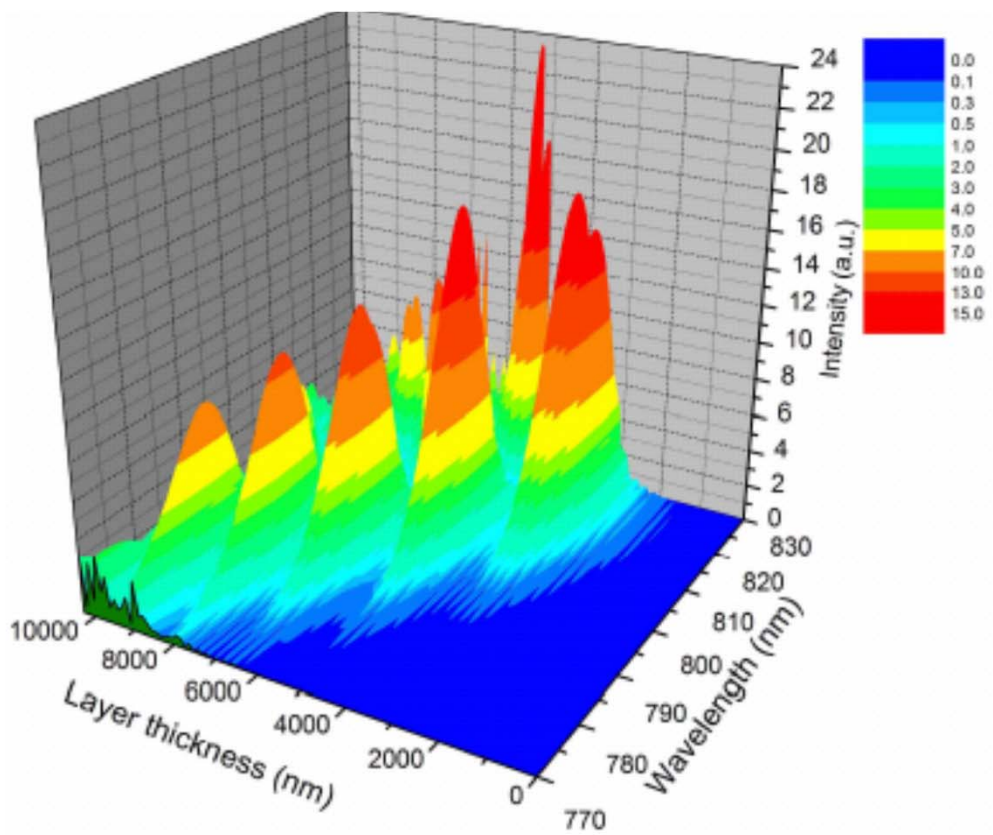


Fig. 6. The penetration depth of spectral components into the HDM structure shown in Fig.1a.
Light enters the structure from the left side.

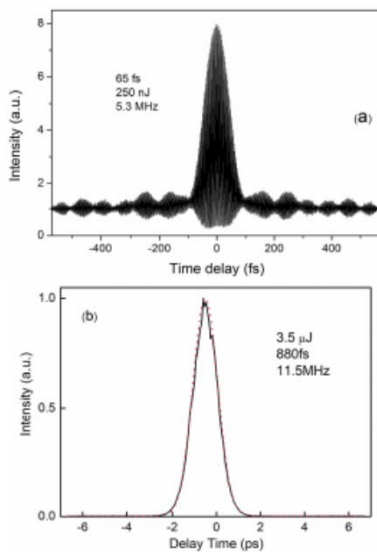
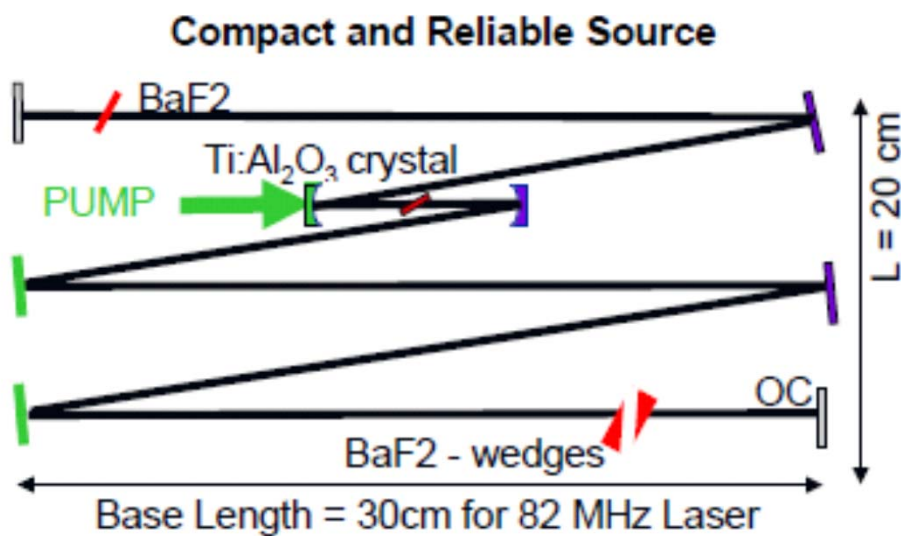


Fig. 7. (a): Interferometric autocorrelation trace of 0.25- μ J pulses delivered by a Ti:Sa CPO and compressed via 20 bounces off the 800-nm HDMs presented above. (b): Intensity autocorrelation trace of 3.5- μ J pulses produced by an Yb:YAG disk oscillator.



5 fs laser design

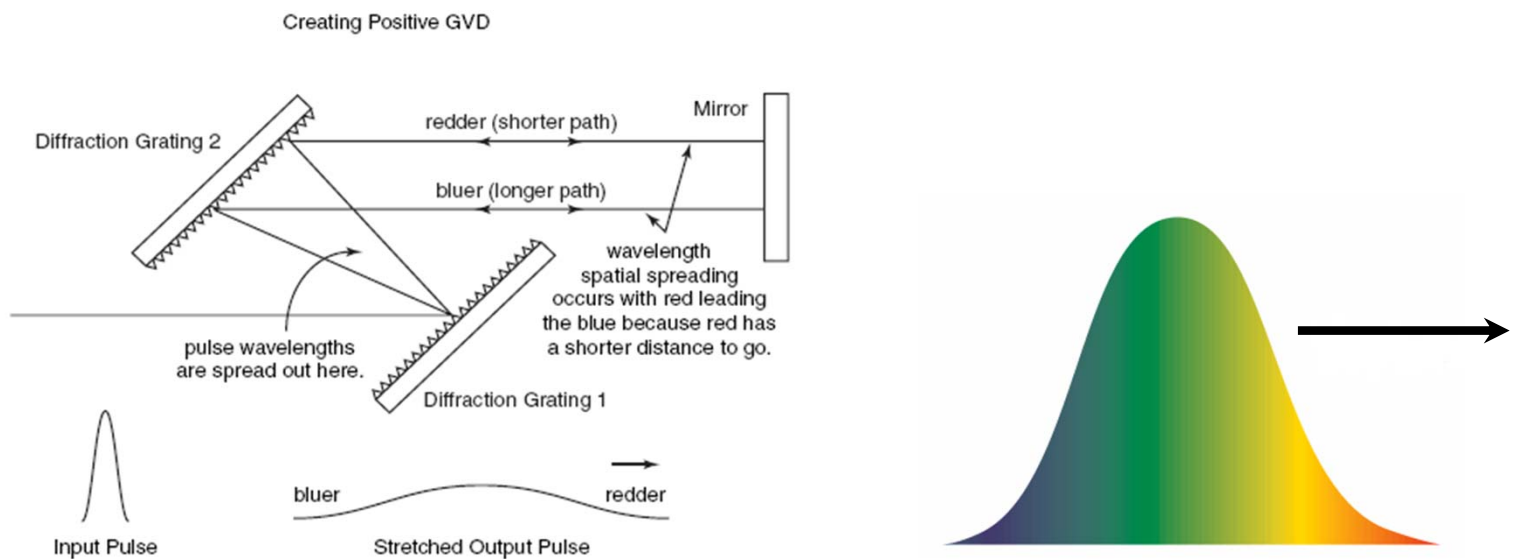
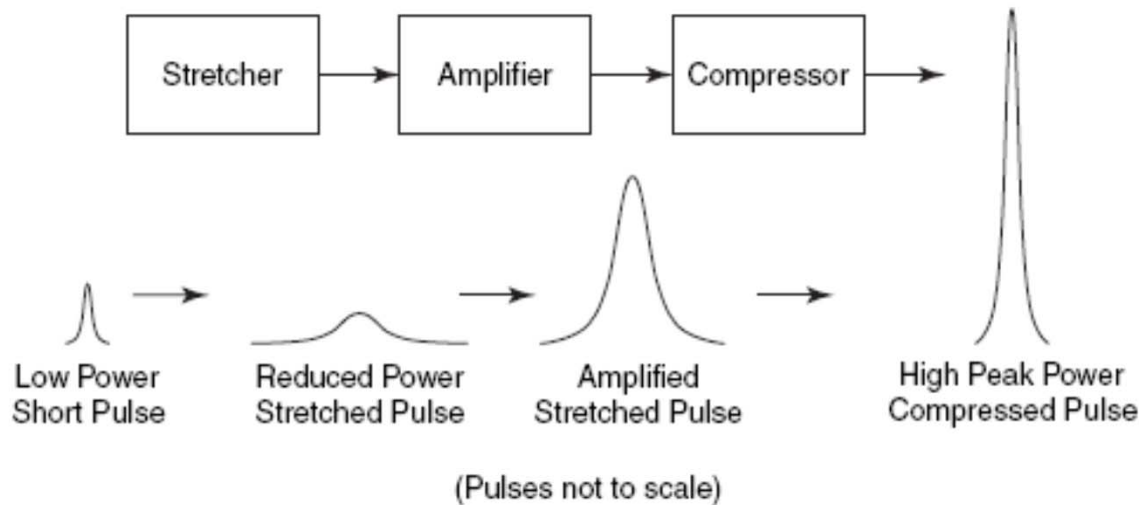


Figure 3-4: Principle of pulse stretching using positive GVD

